A Novel Method for Development of High-strength on 20 Steel Plate by Surface Shot Blasting Treatment and Nitriding

Yongcun Li[1, a], Ping Li[1, b], Ke Wang[1, c] and Weiping Tong[1, d, *]

[1]Northeastern University, Shenyang 110819, China.

[a] YC_Lee1988@163.com
[b] holidaybwping@163.com
[c] wangkewave@163.com
[d] wptong@mail.neu.edu.cn

Abstract. With the impact of 304 stainless steel balls, a plastic deformation layer of submicron grains with abundance defects was produced on the surface of 20 steel by mean of surface shot blasting treatment (SSBT), the thickness of plastic deformation layer is 100 μm and 120 μm for 30 min and 60 min SSBT, respectively. The treated and un-treated spencimens were nitrided in gas nitriding furnace. A $Fe_{2-3}N$ and Fe_4N compound layer formed on the surface of the specimens after nitriding. All compound layers have the similar thickness with different SSBT time. N element has diffused to core of the specimens in the experimental condition of this work, the diffusion layer of specimens contain many granular θ cementite and some needle-like Fe_4N nitride, and the numbers of nitride in 60 min SSBT is much more than that in 30 min treament. The Maximum value of microhardness after 30 min and 60 min treatment nitrided was 823 HV and 802 HV measured on the surface of all treated specimens and then it gradually decreased to the core value as the increase of the depth. The tensile strength of 30 min and 60 min SSBT nitriding specimens is 581 MPa and 627 MPa, respectively. And increased obviously from 397 MPa of the initial specimen.

Keywords: plastic deformation, surface shot blasting treatment, nitriding.

1. Introduction

It is generally known that the material failures occur on surfaces such as fatigue fracture, fretting fatigue, wear and corrosion in most cases, etc. These failures are very sensitive to the structure and properties of the material surface. Therefore, the overall performance and service behavior of material can be enhanced though improve of the microstructure and properties of surface by preparation of nano-materials with unique structural features and a series of excellent performance [1-4]. Some techniques such as rapid solidification, high pressure torsion [5, 6], sliding wear [7], mechanical milling [8, 9], ball drop [10] and shot peening [11] have investigated to produce the nanostructured

crystals. Different microstructures can be obtained within the deformed surface layer from the treated surface to the strain-free matrix by surface mechanical attrition treatment (SMAT). This technique has been successfully introduced in achieving surface Nano crystallization (SNC) in different materials including pure metals, alloys and steels [12, 13]. Tong et al. [14] had demonstrated low temperature nitriding (400 ℃) of 38CrMoAl steel subjected to SMAT. The experimental investigations of Wang et al. [15] had demonstrated that the Nano grains have thermal stability up to 450 ℃. In nanocrystalline and ultra-fine grained materials, the presence of large number of grain boundaries and triple junctions could act as fast atomic diffusion channels [16, 17]. In the past decade, diffusion behavior in nanostructured or ultra-fine grained materials produced by severe plastic deformation (SPD) has become an attractive topic, since SPD processing is a promising route for producing bulk nanostructured materials with enhanced properties [18, 19].

In the current works, the study of nanocrystallization on the surface of the material is mainly in the laboratory stage, the applications in industry are heavily restricted. In this paper, a new method is used for surface nanometerization which is suitable for the materials of complex shapes and large size-surface shot blasting treatment (SSBT) technology. Surface plastic deformation and gas nitriding are applied to 20 steel. The microstructure and the mechanical properties of the 20 steel were investigated.

2. Experimental

A commercial 0.2 wt% low carbon steel (named 20 steel) plate of 1.5 mm thick, with a composition (wt.%) of 0.2 C, 0.20 Si, 0.50 Mn, 0.20 Cr, 0.10 Ni and Fe (residue) was used for the investigation. The 20 steel was machined into 30 x 20 mm. The specimens were mechanically gritted with silicon carbide paper and polished to a mirror surface. Prior to the nitriding process, plastic deformation was carried out in shot blasting equipment, the schematically diagram illustrating of the SSBT equipment was shown in Fig.1. The specimens were processed for 30 min and 60 min both side alternative with a motor frequency at 800 $r \cdot min^{-1}$ using 304 stainless steel balls of 4 mm diameter, the diameter of electromotor vane is 350 mm, so the estimated velocity of the 304 stainless steel balls is about 29.3 $m \cdot s^{-1}$. The specimens were cleaned in ethanol before nitriding. The nitriding atmosphere is high purity ammonia (99.95 wt.%) of gas pressure as 1atm, ammonia decomposition rate is 30-40 %, the nitriding temperature is 500 ℃ with the heating rate of 10 ℃·min-1 holding 50 h. All specimens were ultrasonically cleaned in water and ethanol before characterization. Cross-sectional specimens for optical microscope and SEM investigation were prepared by grinded from 320 to 2000 grit papers and metallographically polished with 1 μm diamond polishing paste subsequently ultrasonically cleaned and etched by a reagent of 4 vol.% nital. An optical microscope (OM) OLYMPUS-GX71 and field emission scanning electron microscopy Ultra Plus (ZEISS) were employed for the microstructure examination. The phase components of the spciments were determined by X' Pert Pro PW3040/60 X-ray diffractometer (XRD) using monochromated Cu Kα radiation.

Mechanical properties of the specimens were surveyed according to microhardness and tensile strength at room temperature. The microhardness profiles were obtained by a Vickers hardness tester using 200 g load for 10 s. The tensile test was tested in the universal testing machine (IDW-200H) at a crosshead speed of 60 $\mu m \cdot min^{-1}$. The tensile strength is measured following:

$$\tau = \frac{F_b}{A} \quad (1)$$

Where τ = tensile strength (MPa), F_b= maximum load (N), A=cross-sectional area (mm^2).

Each value above all is the average of 5 measurements under the same condition.

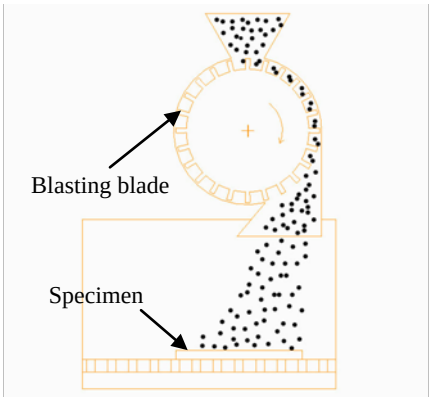

Fig. 1 Schematic diagram illustrating of SSBT machine.

3. Result and discussion

The OM micrographs of cross section and core microstructure after 30 min and 60 min SSBT nitriding were shown in Fig. 2(a), (c) and Fig. 2(b), (d), respectively. The inset backscattered electron image is the enlarged view of cross section. A plastic deformation layer with different thickness on the surface of specimens was formed after 30 min and 60 min SSBT, the grain size is 0.5-5 μm in plastic deformation layer which has been refined. The thickness of the plastic deformation layer is about 100 μm and 120 μm, respectively. A continuous white bright compound layer of about 30 μm thickness was observed in both treatment handing. The upper part of the complex compound layer shown intermittent morphology after nitriding because it including ε-$Fe_{2\text{-}3}N$ and γ′-Fe_4N, the ε-$Fe_{2\text{-}3}N$ is brittleness phase which was easy broken among specimen preparation process. The consecutive white bright compound layer is γ′-Fe_4N phase with the thickness of 15 μm.

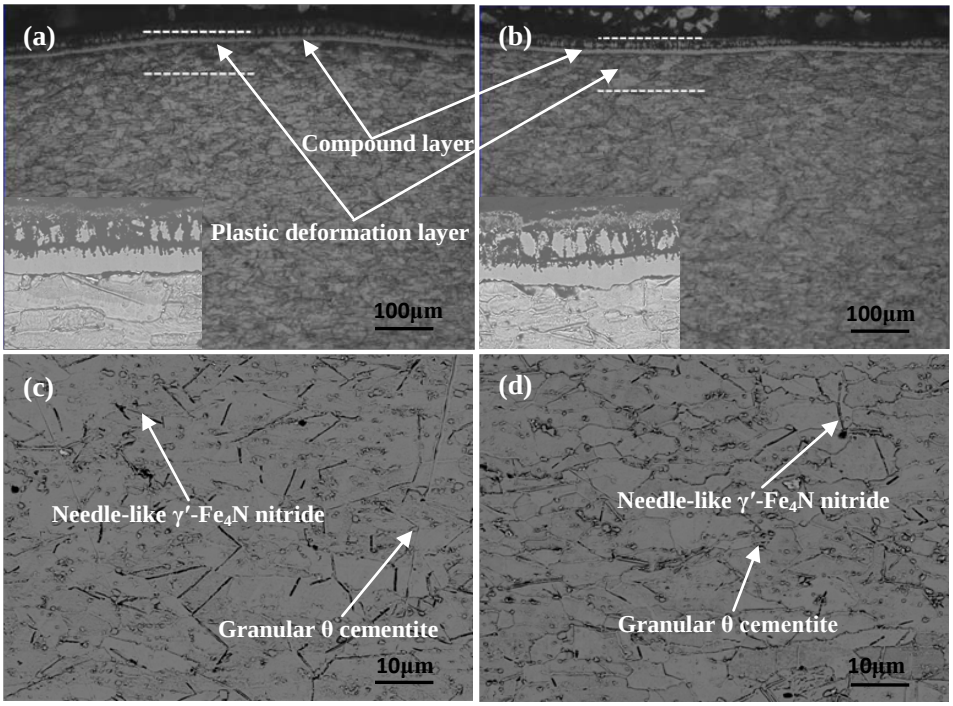

Fig. 2 OM micrograph and backscattered electron image of cross section and core microstructure after SSBT and nitriding for various durations.

A diffusion layer occurred under the compound layer as shown in Fig. 2(c) and Fig. 2(d). In the experimental condition of this paper, N element had diffused into the core structure of the 1.5 mm specimens. It should be attributed to the singularity behavior of refined grain structure by SSBT on specimens. The microstructural characterization of the SSBT 20 steel specimens indicated a high concentration of the non-equilibrium defects (dislocations and subgrain boundaries) in the sub-surface layer that are induced by plastic deformation. These defects may decrease the activation energy of diffusion and act as fast atomic transfer channels. Similar kinetics enhancement can be accomplished for the diffusion zones obtained in the nitriding process. The diffusion layer of specimens contains many of granular θ cementite and some needle-like γ′-Fe_4N nitride, as shown in Fig. 2(c) and Fig. 2(d), the grain size was measured as 2-10 μm. The numbers of γ′-Fe_4N phase in 60 min SSBT was larger than 30 min SSBT, and decreased obviously with the increasing depth from the surface.

The SEM morphologies and map scanning for the composition distribution of the section of the 20 steel after 60 min SSBT nitriding were shown in Fig. 3. There is a certain amount distribution of N element in core of specimens. The compound layer consists of ε-$Fe_{2\text{-}3}N$ and γ′-Fe_4N, as a result, N element has the more concentration than core microstructure. The upper part of the compound layer shows rubble shape because of the brittle ε-$Fe_{2\text{-}3}N$ phase. In the white bright layer, density-hard γ′-Fe_4N phase has the higher content of Fe and N element.

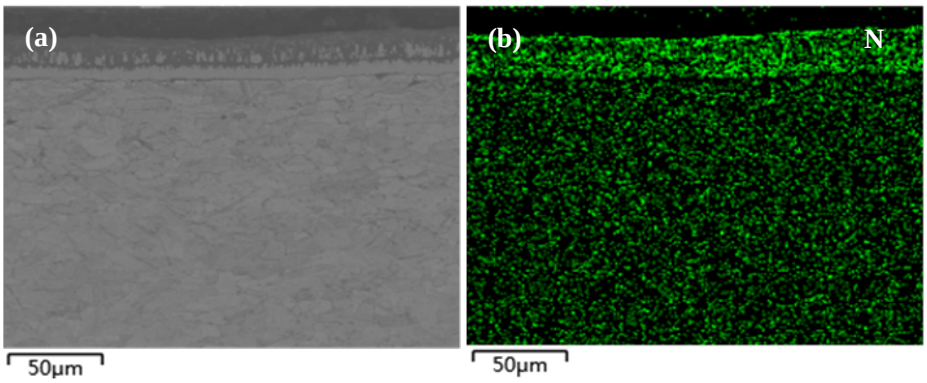

Fig. 3 Element distribution of N element on cross section after 60 min SSBT and nitriding (a) secondary electron image, (b) N distribution image.

The Fig.4 shows the X-ray diffraction patterns of 20 steel initial sample and the samples treated by SSBT for 30 min and 60 min, it provides information on about 5 μm thick phase composition from the nitrided surface. The specimen contains α-Fe diffraction peaks reduced, the ε-$Fe_{2–3}N$ and γ'-Fe_4N diffraction peaks appeared after SSBT 30 min and nitriding process. After SSBT 60 min nitriding, the diffraction peaks of the ε-$Fe_{2–3}N$ and γ'-Fe_4N phases obviously increase and the diffraction peaks of α-Fe phase completely disappeared, indicating a substantial enhancement of the volume fraction of nitrides in the surface layer. It means a thick enough compound layer in the surface of the sample formed in the conditions of this experiment in the X-ray inspection range.

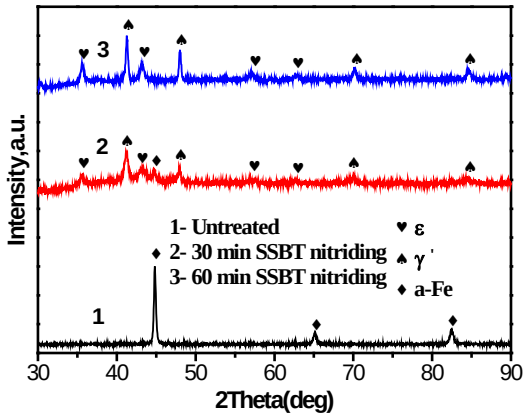

Fig. 4 XRD patterns obtained from the surface of original specimen the specimens after SSBT and nitriding for different treatment processes.

Fig. 5 depicts the variation of microhardness from the treated surface to the bulk material. Maximum value of microhardness after 30 min and 60 min SSBT nitriding was 823 HV and 802 HV measured at the surface of all treated specimens and then it gradually decreased to the core value as the increase of the depth. But the specimen treated by SSBT still keep higher hardness in the depth of 120μm from the surface (above 400 HV), while the hardness of the untreated nitride specimen decreases more rapidly along the increase of the depth. Case depth after nitriding is a matter of convention. The reason of this phenomenon can be explained as the fine-grained nitride on the surface, the crystal grain on the surface reach sub-micron scales by SSBT, the proportion of grain boundary increased dramatically, which act as the fast path for the atomic diffusion, make the nitrogen atoms diffusion much more easier.

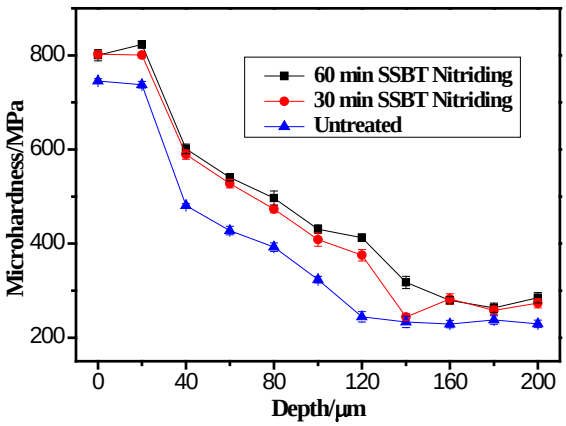

Fig. 5 Microhardness curves of the specimens with different treatment processes.

The Fig. 6 is the tensile stress strain curves of the initial specimen and the 30 min and 60 min SSBT nitriding specimens. The yield strength and tensile strength of treated specimens are both higher than those initial 20 steel specimens. And the tensile strength of 30 min and 60 min SSBT nitriding specimen is 581 MPa and 627 MPa, respectively, which is obviously increased from 397 MPa of the initial specimen. The elongation decreases from 61% to 40.8% and 40.1%. The nitriding process can improve the surface strength of materials, so the overall performance of the material has been improved. But the good plasticity didn't decreased dramatically. Generally, it is hard to get both high strength and high plasticity at the same time, and the both high quality can’t be observed at the same time by traditional chemical heat treatment. In this paper, the high strength and high plasticity of the samples after SSBT and nitriding process may advance the process of the industrialization.

The plasticity of SSBT nitriding specimens have been maintained well (40.8 %), owe to the existence of many sub-micron nitrogen particles. These particles not only obstructed the movement of dislocation, also inhibited the initiation and expansion of cracks. As plastic deformation occurs, the cracks deflected when they impact the nitrogen particles, its shape and length changed, mean that they need absorb additional energy to generate a new fracture [20].

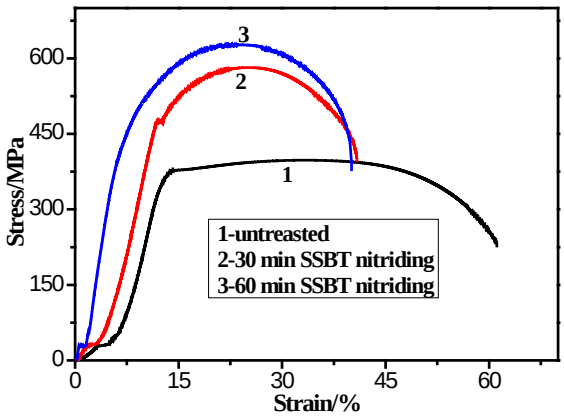

Fig. 6 Tensile test stress-strain curves for the specimens with different treatment time nitriding and for the untreated specimen.

4. Conclusions

1. With the impact of 304 stainless steel balls, a plastic deformation layer of submicron grains with abundance defects was produced on the surface of 20 steel by SSBT, the thickness of plastic deformation layer is 100 μm and 120μm for 30 min and 60 min treatment, respectively.

2. A $Fe_{2\text{-}3}N$ and Fe_4N compound layer formed on the surface of the specimens after nitriding. All compound layers have similar thickness with different SSBT time. N element has diffused to core of the specimens in the experimental condition, the diffusion layer of specimens contain many granular θ cementite and some needle-like γ′-Fe_4N nitride, and the numbers of nitride in 60 min SSBT is much more than that in 30 min SSBT.

3. The microhardness and tensile strength were measured at room temperature. Maximum value of microhardness after 30 min and 60 min SSBT nitriding is 823 HV and 802 HV measured at the surface of all treated specimens and then it gradually decreased to the core value as the increase of the depth. The tensile strength of 30 min and 60 min SSBT nitriding specimens is 581 MPa and 627 MPa, respectively. And it increased obviously from 397 MPa of the initial specimen.

5. References

1. K. Lu, J.T. Wang, A new method for synthesizing nanocrystalline alloys. J. Appl. Phys. 69 (1991) 522- 524.
2. J.Y. Suh, D.H. Bae, Mechanical properties of Fe-based composites reinforced with multi-walled carbon nanotubes. Mater. Sci. Eng. A. 582 (2013) 321-325.
3. J.F. Gu, D.H. Bei, K. Lu, et al. Improved nitrogen transport in surface nanocrystallized low-carbon steels during gaseous nitridation. Mater Lett. 55 (2002) 340-343.
4. Z.B. Wang, N.R. Tao, S. Li, W. Wang, J. Lu, K. Lu. Effect of surface nanocrystallization on friction and wear properties in low carbon steel, Mater. Sci. Eng. A. 352 (2003) 144-149
5. A.P. Zhilyaev, T.G. Langdon, Using high-pressure torsion for metal processing: Fundamentals and

applications, Prog. Mater. Sci. 53 (2008) 893-979.

6. V.V. Tcherdyntsev, S.D. Kaloshkin, D.V. Gunderov, E.A. Afonina, I.G. Brodova,V.V. Stolyarov, Yu. V. Baldokhin, E.V. Shelekhov, I.A. Tomilin, Phase composition and microhardness of rapidly quenched Al–Fe alloys after high pressure torsion deformation, Mater. Sci. Eng. A. 375-377 (2004) 888-893.
7. D.A. Hughes, N. Hansen, Graded nanostructures produced by sliding and exhibiting universal behavior, Phys. Rev. Lett. 87 (2001) 135503–135511.
8. J.Y. Huang, Y.K. Wu, H.Q. Ye, Deformation structures in ball milled copper, Acta Mater. 44 (1996) 1211-1221.
9. M. Umemoto, B. Huang, K. Tsuchiya, N. Suzuki, Formation of nanocrystalline structure in steels by ball drop test, Scripta Mater. 46 (2002) 383.
10. M. Umemoto, K. Todaka, K. Tsuchiya, Formation of nanocrystalline structure in carbon steels by ball drop and particle impact techniques, Mater. Sci. Eng. A. 375–377 (2004) 899-904.
11. G. Liu, S.C. Wang, X.F. Lou, J. Lu, K. Lu, Low carbon steel with nanostructured surface layer induced by high-energy shot peening, Scripta Mater. 44 (2001) 1791-1795.
12. Estrin Y, Vinogradov A, Extreme grain refinement by severe plastic deformation: A wealth of challenging science, Acta Mater. 61 (2013) 782-817.
13. HH. Liebermann, Rapidly solidified alloys: Processes, structures, properties, applications, New York, NY: Marcel Dekker, 1993.
14. W.P. Tong, Z. Han, L.M. Wang, J. Lu, K. Lu, Low-temperature nitriding of 38CrMoAl steel with a nanostructured surface layer induced by surface mechanical attrition treatment, Surf. Coat. Technol. 202 (2008) 4957–4963.
15. G.M. Wang, A. Calka, S.J. Campbell, W.A. Kaczmarek, Carburization of iron by ball-milling Fe50C50, Mater. Sci. Forum. 179-181 (1995) 201-206.
16. H. Gleiter, Nanocrystalline materials, Prog. Mater. Sci. 33 (1989) 223-315.
17. K. Lu, Nanocrystalline metals crystallized from amorphous solids: nanocrystallization, structure, and properties, Mater. Sci. Eng. R. 16 (1996) 161-221.
18. R.Z. Valiev, T.G. Langdon, Principles of equal-channel angular pressing as a processing tool for grain refinement, Prog. Mater. Sci. 51 (2006) 881.
19. R.Z. Valiev, M.J. Zehetbauer, Y. Estrin, H.W. Hoppel, Y. Ivanisenko, H. Hahn, G.Wilde, H.J. Roven, X. Sauvage, T.G. Langdon, The innovation potential of bulk nanostructured materials, Adv. Eng. Mater. 9 (2007) 527-533.
20. H. Somekawa, T. Mukai, Effect of grain refinement on fracture toughness in extruded pure magnesium, Scripta Mater. 53 (2005) 1059-1064.